Nonlinearities in modified gravity cosmology — II. Impacts of modified gravity on the halo properties

Youcai Zhang[1],* Pengjie Zhang[1], Xiaohu Yang[1], and Weiguang Cui[2]
[1]*Key Laboratory for Research in Galaxies and Cosmology, Shanghai Astronomical Observatory; Nandan Road 80, Shanghai 200030, China; E-mail: yczhang@shao.ac.cn and*
[2]*Astronomy Unit, Department of Physics, University of Trieste, via Tiepolo 11, I-34131 Trieste, Italy*

The statistics of dark matter halos is an essential component of understanding the nonlinear evolution in modified gravity cosmology. Based on a series of modified gravity N-body simulations, we investigate the halo mass function, concentration and bias. We model the impact of modified gravity by a single parameter ζ, which determines the enhancement of particle acceleration with respect to GR, given the identical mass distribution ($\zeta = 1$ in GR). We select snapshot redshifts such that the linear matter power spectra of different gravity models are identical, in order to isolate the impact of gravity beyond modifying the linear growth rate. At the baseline redshift corresponding to $z_S = 1.2$ in the standard ΛCDM, for a 10% deviation from GR($|\zeta - 1| = 0.1$), the measured halo mass function can differ by about $5 - 10\%$, the halo concentration by about $10 - 20\%$, while the halo bias differs significantly less. These results demonstrate that the halo mass function and/or the halo concentration are sensitive to the nature of gravity and may be used to make interesting constraints along this line.

PACS numbers: 98.80.-k; 98.65.Dx; 95.36.+x

I. INTRODUCTION

Dark matter halos are prominent structures in the dark universe. Their abundance, density profile and clustering (halo bias) contain valuable cosmological information. In particular, dark matter halos form and grow under gravitational instability. Hence halo properties contain rich information on the nature of gravity at $\sim$ Mpc scales and above, and can provide strong gravity constraints [1–17]. These properties also provide a powerful tool to understand the matter clustering through the halo model [18, 19], which is also a sensitive measure of gravity.

In [20] (hereafter paper I) we run a controlled set of N-body simulations with identical initial condition to study the impact of modified gravity (MG) on the matter power spectrum. These simulations adopt a MG parameterization with a single parameter ζ. ζ is the relative enhancement of nonrelativistic particle acceleration with respect to general relativity (GR), given the identical mass distribution. More specifically, it is the quantity that enters into the ψ-ρ relation in Fourier space,

$$k^2\psi = -\zeta 4\pi G a^2 \delta\rho \ . \tag{1}$$

Here, $\delta\rho \equiv \rho - \bar{\rho}$ and ρ is the matter density. ψ is defined through $ds^2 = -(1+2\psi)dt^2 + a^2(1+2\phi)d\mathbf{x}^2$. ψ is the only gravitational potential that nonrelativistic particles can sense. So the value of $\zeta(k, z)$ as a function of scale and redshift, along with the initial condition and the expansion rate of the universe, completely fixes the evolution of the matter density and velocity fields. This is the major reason that we adopt this single parameter parametrization on modified gravity N-body simulations. For more detailed discussion on this parametrization, please refer to paper I.

Neverthless, such parameterization is highly simplified in the sense that it lacks any screening mechanism [17] required to pass the solar system tests. For this reason, these simulations lose the capability to explore the rich consequences induced by the MG environmental dependence. These features have been explored in advanced simulations on $f(R)$ and DGP [14, 21–26]. Nevertheless, our simulations benefit from costing no extra time than the ordinary CDM simulations. So in principle one can run a large number of such simulations within reasonable amount of time to fairly sample relevant parameter space. One then interpolates/extrapolates the simulation results to explore the whole relevant parameter space and understand the nonlinear evolution for ζ of general spatial and time dependence. The hope is that, by choose appropriate spatial and time dependence in ζ, one can effectively take the environmental dependence into account [51].

In the current paper, we will examine the halo properties in these simplified MG simulations, including the halo abundance, concentration and bias as a function of mass and redshift. In the standard framework of structure formation in GR, these properties, in particular the halo abundance and bias, are largely fixed by the linear matter power spectrum at the corresponding epoch. We utilize this property to better isolate the impact of MG. We will compare the above properties not at the same redshift, but at redshifts of identical linear matter power spectrum. The same method is also adopted in paper I. It has extra benefit of reducing cosmic variance and numerical artifact, since we focus on the differences between

*Electronic address: yczhang@shao.ac.cn

different MG simulations with identical initial condition.

This paper is organized as follows. We briefly describe our simulations in §II and present results in §III. We discuss and summarize in §IV.

II. N-BODY SIMULATION

We run a set of simulations with the TreePM parallel code GADGET-2 [27] at Shanghai Astronomical Observatory. All the simulations evolved 512^3 dark matter particles in a periodic box of $300\,h^{-1}$Mpc on a side. The cosmological parameters used in the simulations are $\Omega_{\rm m} = \Omega_{\rm dm} + \Omega_{\rm b} = 0.276$, $\Omega_{\rm b} = 0.046$, $h = 0.703$, $\Omega_\Lambda = 0.724$, $n = 1$, and $\sigma_8 = 0.811$. The particle mass and softening length are $1.541 \times 10^{10}\,h^{-1}{\rm M}_\odot$ and $12.89\,h^{-1}$kpc, respectively. Glass-like cosmological initial conditions were generated at redshift $z = 100$ using the Zel'dovich approximation.

In this paper as in Paper I, the modified gravity model is characterized by a single parameter ζ, which determines the enhancement of particle acceleration with respect to GR, given the identical mass distribution ($\zeta = 1$ in GR). All the simulations for different ζ values have the same linear power spectrum, such that

$$P_L(k; z_S, \zeta = 1) = P_L(k; z_\zeta, \zeta), \tag{2}$$

where P_L is linear matter power spectrum, z_S and z_ζ denote the redshifts in the standard ΛCDM and the MG cosmology, respectively. Since all the simulations begin with the identical initial condition, the above relation means that

$$D(z_S, \zeta = 1) = D(z_\zeta, \zeta), \tag{3}$$

where $D(z, \zeta)$ is the linear density growth factor. Given redshifts z_S in the ΛCDM, through Eq. (3) we can calculate the corresponding redshifts z_ζ, which are shown in Table I of Paper I. In this paper, we mainly focus on the redshift $z_S = 1.2$ in the ΛCDM and the corresponding redshifts in the MG universe (10th row of Table I in Paper I).

Dark matter halos were identified from the simulation at each snapshot using the standard friends-of-friends (FOF) algorithm[28] with a linking length of $b = 0.2$ times the mean interparticle separation. For currently favored cosmologies, 15-20% of $b = 0.2$ FOF halos have irregular substructure or have two or more major halo components linked together[29]. Only isolated, relaxed halos are well-fit by the Navarro-Frenk-White (NFW) profile[30], therefore, we use the virial halo mass to fit NFW profile in the simulations. The mass M_{200} is defined as the interior mass within a sphere of radius R_{200} centered on the most bound particle of the halo, where R_{200} is the radius within which the over-density is $\Delta_{200} = 200$ times the mean density $\rho_{\rm mean}$ of the universe. Thus, the mass and radius of a halo are related by

$$M_{200} = \frac{4}{3}\pi\Delta_{200}\rho_{\rm mean}R_{200}^3, \tag{4}$$

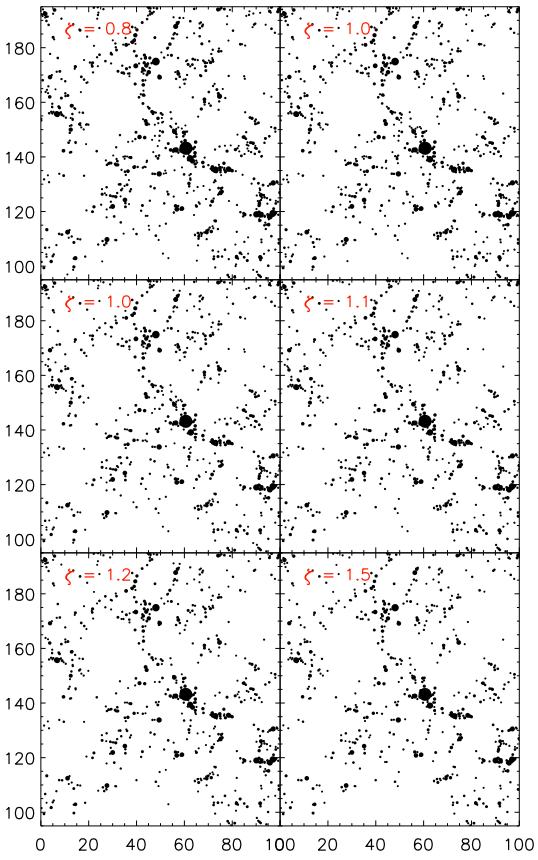

FIG. 1: Comparison of halo distributions from N-body simulations for different ζ values at the baseline redshift $z_S = 1.2$, which is that of $\zeta = 1$ (ΛCDM). The panels show the dark matter halos with the mass $M_{200} \geq 10^{11.5}\,h^{-1}{\rm M}_\odot$ in slices $100 \times 100 \times 8h^{-1}$Mpc, and the sizes of the dots are proportional to the radii R_{200} of the halos.

where $\rho_{\rm mean}$ is the mean density of the universe at redshift z. Note that some authors use a value $\Delta_{\rm vir}$ motivated by the spherical collapse model, where the corresponding radius is specified as $R_{\rm vir}$. This value is both redshift and gravity dependent. It gives $\Delta_{\rm vir} = 339.5$ at $z = 0$ and 178 at $z \gg 1$ for our adopted ΛCDM parameters [31]. It also shows significant deviation in MG models [14]. Since we will compare the halo properties of different MG models at different redshifts (e.g. z_s vs. z_ζ), this latter choice could mix the impact of background cosmology with the impact of gravity. For this reason, we will not adopt this latter definition. Unless otherwise specified, throughout the paper we use a fixed value $\Delta = 200$ to define the halo mass.

Fig. 1 shows the distributions of dark matter halos with the mass $M_{200} \geq 10^{11.5}\,h^{-1}{\rm M}_\odot$ in a slice of thickness $8h^{-1}$Mpc for different ζ values at the baseline redshift $z_S = 1.2$, which is that of $\zeta = 1$ (ΛCDM). According to visual inspection, the general appearances of the large-scale structures are remarkably similar, as a result

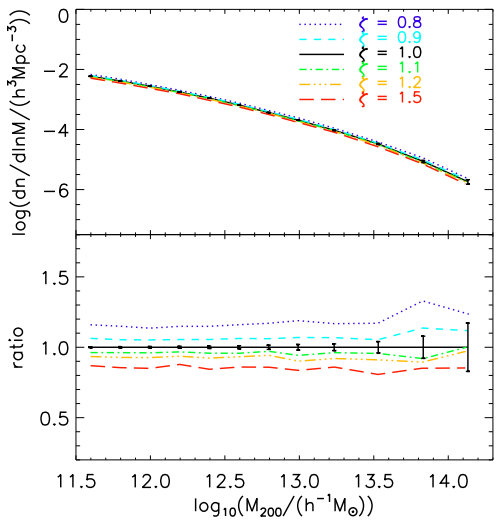

FIG. 2: Measured halo mass functions from N-body simulations for different ζ values at redshift z_ζ where the linear matter power spectrum is identical to that in ΛCDM ($\zeta = 1$) at the baseline redshift $z_S = 1.2$. Since all simulations begin with the identical condition, the measured halo mass function has similar Poisson error. Hence we only show the Poisson error bars of ΛCDM to demonstrate the measurement uncertainty. The lower panel shows the ratio of the measured mass functions of MG models to the one in ΛCDM when they have the same linear power spectrum. The plotted errors are the same Poisson errors showing in the upper panel. Since the Poisson errors of different simulations have strong positive correlations, they largely cancel when taking the ratio. So the plotted errors represent a conservative upper limit of the halo mass function ratio. The lower panel then shows that the observed deviations from a universal mass function are significant.

of the same linear power spectrum for different ζ values. Although the shape of Cosmic Web (the pattern on clusters, filaments, sheets, and voids) is more or less preserved in the $\zeta \neq 1$ runs when compared to the ΛCDM case, we can depict arising differences when looking into the internal properties of dark matter halos.

III. NUMERICAL RESULTS

In this section we show the halo mass function, concentration and bias as a function of M_{200}. Structure grows more slowly in $\zeta < 1$ models than that in GR. So for too low z_S in ΛCDM, structure growth in a $\zeta < 1$ universe may not be able to catch up with that of ΛCDM even at $z_\zeta = 0$ (table I, paper I). For this reason, we only compare the results corresponding to $z_S = 1.2$ in ΛCDM, for which we can compare the halo statistics for all ζ.

A. The halo mass function

One of the long-standing efforts in precision cosmology is to determine the mass function of dark matter halos $\mathrm{d}n/\mathrm{d}M$, which is the number of halos per unit volume per unit mass. It is a sensitive probe of gravity and has been used to put strong constraints on modified gravity models (e.g. [24] on $f(R)$ gravity).

Although the number density of halos of a given mass depends on the shape and amplitude of the power spectrum, analytical work has suggested that the halo abundance can be expressed by a universal functional form when expressed in terms of suitable variables [32–34]. A convenient form to describe halo abundance can be expressed as [35]

$$\frac{\mathrm{d}n}{\mathrm{d}M}(M,z) = f(\sigma)\frac{\rho_0}{M}\frac{\mathrm{d}\,\ln[\sigma^{-1}(M,z)]}{\mathrm{d}M}, \qquad (5)$$

where ρ_0 is the background matter density at redshift $z = 0$, and $\sigma^2(M,z)$ is the variance of the linear matter power spectrum over a length R,

$$\sigma^2(M,z) = \frac{D^2(z)}{2\pi^2}\int_0^\infty k^2 P(k) W^2(kR(M))dk, \qquad (6)$$

where $W(x) = 3[\sin(x) - x\cos(x)]/x^3$ is the Fourier transformation of the top-hat filter, $R(M) = (3M/4\pi\rho_0)^{1/3}$ is the smoothed radius with halo mass M, and $D(z)$ is the growth factor.

This definition of mass function has been widely examined against N-body simulations and useful fitting functions $f(\sigma)$ have been provided by several authors [35–38]. Nevertheless, deviations from the universality have been reported. For example, Bhattacharya et al. [38] found through their N-body simulations that, for their ωCDM cosmological models (where the dark energy equation of state parameter ω is constant in time, but $\omega \neq -1$), the universality of the mass function is systematically broken at a level of 10%. Deviations from the universality are also detected in interacting dark energy models Cui et al. [39]. Cui et al. [39] reported that deviations can exceed $\sim 10\%$ for most of the models in the high mass end.

Fig. 2 shows the measured halo mass functions from our simulations for different ζ values at the baseline redshift $z_S = 1.2$, which is that of $\zeta = 1$ (ΛCDM). The M_{200} halo mass is used in the plot in order to get consistent comparisons with concentration and bias, where the same mass definition are adopted. We have checked our measured halo mass functions for ΛCDM simulation, which agree well with the fitting function proposed by [41].

In order to assess the difference, the Poisson error bars are only added for $\zeta = 1$. Because of the same initial condition been used, the error bars for $\zeta \neq 1$ have the similar forms. In Fig. 2, the lower panel shows the ratio of the measured mass functions of MG models to the one in ΛCDM. The Poisson error bars for $\zeta = 1$ are added to assess the maximum limit. Since $D(z_\zeta, \zeta) = D(z_S, \zeta = 1)$,

the linear power spectrum and hence $\sigma(M,z)$ are identical. If the halo mass function is indeed universal and described by Eq. (5) and Eq. (6), the mass function in the MG model should be the same as that in ΛCDM. However, the result in Fig. 2 shows the difference of mass functions between $\zeta = 0.8$ and $\zeta = 1.0$(ΛCDM) is about 20% with the halo mass range from $10^{11.5}\,h^{-1}\mathrm{M}_\odot$ to $10^{14.0}\,h^{-1}\mathrm{M}_\odot$. The difference between $\zeta = 1.2$ and $\zeta = 1.0$ is about 10%. We find that the difference of $\zeta = 1.2$ is about twice that of $\zeta = 0.8$, although they have the same 20% deviation from GR. For a 10% deviation from GR($\zeta = 0.9$, or $\zeta = 1.1$), the measured mass functions can differ by about $5 - 10$%. Interestingly, the difference of $\zeta = 0.9$ is also about twice that of $\zeta = 1.1$. In general, for the identical deviation of ζ from unity, the deviation of halo mass function of $\zeta < 1$ is about twice that of $\zeta > 1$, which implies that the decrease of gravity can lead to more difference of halo mass function. This behavior can also be found in the bottom-right panel of Fig. 4 in Paper I for the comparison of the nonlinear power spectra. For the same deviation of ζ from unity, the deviation of nonlinear power spectra of $\zeta < 1$ are about twice that of $\zeta > 1$ at $\Delta^2 \sim 10$.

If the halo abundance is completely determined by the shape and amplitude of the linear power spectrum, the halo mass functions for different ζ simulation should have the identical form. However, based on the measured halo mass functions from N-body simulations for different ζ values at the same linear power spectrum, we find that this is not the case, which means that the halo abundance also depends on the structure growth history and the underlying gravity. The deviation of halo abundance becomes larger if the deviation of ζ from unity is larger. The halo mass function is therefore a sensitive probe for our modified gravity model.

B. Halo concentration

The concentration parameter has been widely used to describe the internal structure of halos[42–46]. Recently, Jeeson-Daniel et al. [47] investigated the correlation between nine different dark matter halo properties, and they claimed that while the scale of a halo is set by its mass, the concentration is the most fundamental property. In this paper, the NFW form is used to fit the halo density profiles, which can be approximated by a simple formula with two free parameters,

$$\frac{\rho(r)}{\rho_{\rm mean}} = \frac{\delta_{\rm c}}{(r/r_s)(1+r/r_s)^2}, \tag{7}$$

where r_s is a scale radius and $\delta_{\rm c}$ is a characteristic density contrast. The concentration of a halo is defined as $c = R_{200}/r_s$, thus $\delta_{\rm c}$ and concentration are linked by the relation

$$\delta_{\rm c} = \frac{200}{3}\frac{c^3}{[\ln(1+c) - c(1+c)]}. \tag{8}$$

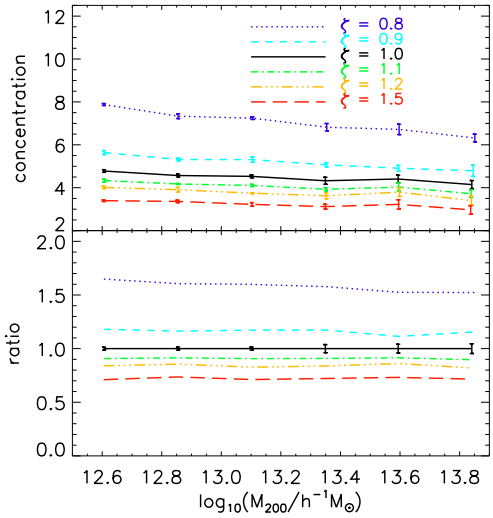

FIG. 3: Measured halo concentrations from N-body simulations for different ζ values at the baseline redshift $z_S = 1.2$. The lower panel shows the ratio of the measured halo concentrations of MG models to the one in ΛCDM. For clarity, we plot the error bars of the $\zeta = 1$ result. As explained in Fig. 2, these errors are conservative upper limit. Hence the observed differences in c are statistically significant. Difference in the nature of gravity contributes to these differences. However, since $z_S \neq z_\zeta$, difference in c also arises from difference in the background matter density. More systematical studies are required to disentangle the two and to infer the nature of gravity from the halo concentration.

In our calculation of concentration from the simulation, the radius of a halo is divided in uniform logarithmic bins ($\Delta \log_{10} = 0.1$), starting from the radius where the bin contains at least 20 particles to $R_{\rm max} = R_{200}$ (or to $R_{\rm vir}$ in case halo masses are defined using the over-density $\Delta_{\rm vir}$). Due to the relation of equation 8, at given halo mass M_{200}, there is a single free parameter in equation 7, which can be expressed as the concentration parameter c. The best-fit concentration parameter can be computed from simulation by minimizing the rms deviation σ between the binned $\rho(r)$ and the NFW profile,

$$\sigma^2 = \frac{1}{N_{\rm bins}}\sum_{i=1}^{N_{\rm bins}}[\log_{10}\rho_i - \log_{10}\rho_{\rm NFW}(c)]^2\,. \tag{9}$$

Fig. 3 shows the measured concentration of the halos contained at least 200 particles for different ζ values. In each mass bin, the halos are randomly divided into five parts. Then the average concentration of each part is calculated. The error bars plotted in Fig. 3 is the standard deviation of five average concentrations. In general the errors of the average concentrations of the total halos can be reduced by a factor of $\sqrt{5}$. For $\zeta = 1$, we find that the concentrations of halos with $N > 1000$ particles ($M_{200} > 13.18\,h^{-1}\mathrm{M}_\odot$) can be approximately fitted by a power law $c \propto M_{200}^{-0.1}$, which is in good agreement with the results of Neto et al. [45]. For the halos with

$N < 1000$ particles, we find the power law index is less than -0.1, which is in good agreement with the results calculated by the model of Zhao et al. [46] [52].

Because the main focus in this paper is to compare the difference of concentration for different ζ values, in the lower panel of Fig. 3, the ratio of the measured halo concentrations is plotted. For a 10% deviation from GR ($|\zeta - 1| < 0.1$), the deviation of halo concentration can differ by $10-20\%$, which means that the modified gravity can significantly affect the structure formation on small scale and the internal properties of the dark matter halos. For $\zeta = 0.8$, the deviation of halo concentration even differ by larger than 50% compared to that of $\zeta = 1.0$. Here again, with similar difference in ζ, the concentration difference of $\zeta < 1$ is much larger than that of $\zeta > 1$.

The discrepancy between the different ζ values is mainly due to the different background density although they have the same linear matter perturbation. Since structure grows faster in $\zeta > 1$ cosmology ($z_\zeta > z_S$), halos in this universe form in a background with higher mean density ($\propto (1+z)^3$). We then expect them to have a smaller concentration[46]. For the same reason, we expect halos with $\zeta < 1$ have a larger concentration. The behavior of the concentrations for different ζ values is roughly similar to the trend of the concentrations corresponding to the redshift z_ζ in ΛCDM models. Large values of the ratio of the concentration parameters from unity implies that the halo concentration is a valuable property to detect different modified gravity models.

C. Halo bias

We define the bias of dark matter halos as the ratio of the halo mass cross-power spectrum to the dark matter power spectrum

$$b(k, M_{200}) = \frac{P_{hm}(k, M_{200})}{P_{mm}(k)}, \tag{10}$$

where $P_{hm}(k, M)$ denotes the cross-power spectrum with halos of mass M_{200}, and $P_{mm}(k)$ is the dark matter power spectrum. This measure dose not require a shot-noise correction, and it yields better statistics when the halos become sparse. The power spectrum is calculated using Daubechies wavelet mass assignment, which avoids the sampling effect. Although halo bias is scale dependent in the quasi-linear and nonlinear regime, here we focus on the large-scale bias, where b is independent of k. We calculate b as the average over the 5 largest wavelength modes ($k \lesssim 0.1h$/Mpc) in the simulation. We also check these results against bias as defined by $b_{hh} = \sqrt{P_{hh}/P_{mm}}$, and we find that there is a good agreement between b_{hm} and b_{hh}.

In the ΛCDM cosmological model, the linear halo bias can be expressed as a function of ν, [41, 48–50], where $\nu = \delta_c/\sigma$ is the ratio of the critical over-density required for collapse to the rms density fluctuation.

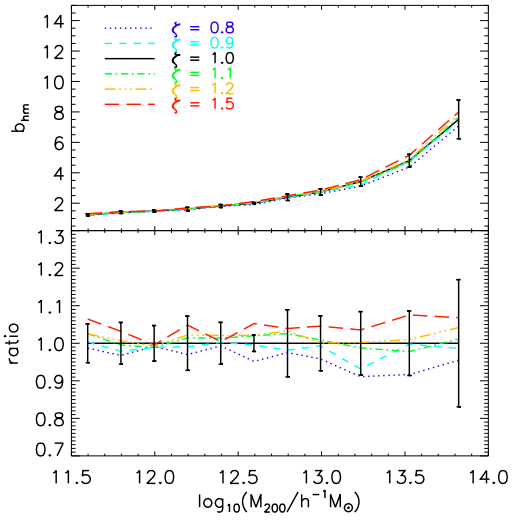

FIG. 4: Measured halo bias from N-body simulations for different ζ values at the baseline redshift $z_S = 1.2$. The lower panel shows the ratio of the measured halo bias of MG models to the one in ΛCDM. As in previous plots, the errors are that of ΛCDM. As explained in previous plots, these errors are conservative upper limit. For this reason, the observed difference in the halo bias is statistically significant, despite the apparently large error bars.

Fig. 4 shows measured halo biases from N-body simulations for different ζ values at the baseline redshift $z_S = 1.2$. The error bars is the standard deviation of the 5 largest wavelength modes. The error bars for different ζ values have very similar amplitude and only $\zeta = 1.0$ has been plotted in the figure. The lower panel shows the ratio of the measured halo bias of MG models to the one in ΛCDM. We find that the difference of halo bias for different ζ values becomes larger as the increase of halo mass. However, the deviations of halo bias differ by less than 10% from GR ($\zeta = 1$) for all the $\zeta \neq 1$ values used in our simulation. This behavior is expected due to the halo bias is a function of ν in ΛCDM model. The simulations for different ζ values have the same linear power spectrum and growth factor, therefore, according to Eq. (6) they have the same density fluctuation σ. Besides δ_c is weakly dependent on the redshift, thus the difference of the halo bias for different ζ values is very small. We can conclude that the halo bias is a weak statistics to detect the modified gravity model.

IV. DISCUSSION AND CONCLUSION

In this paper we have compared the halo mass function, concentration and bias based on a series of modified gravity N-body simulations. The modified gravity model is characterized by a single parameter ζ, which determines the enhancement of particle acceleration with respect to GR. All the simulations for different ζ values are

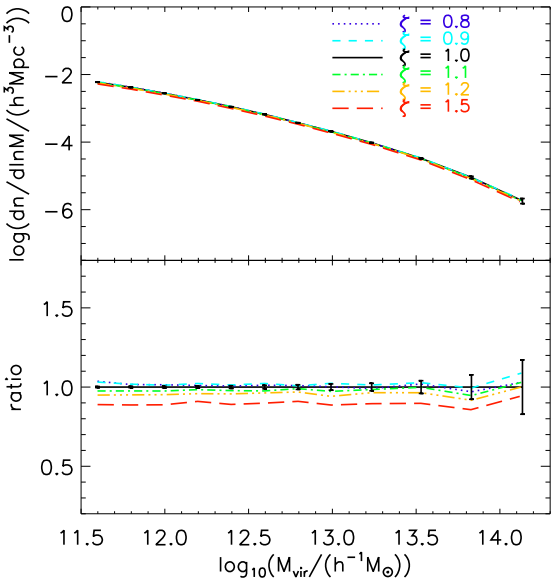

FIG. 5: Same as Fig. 2 but for the virial halo mass $M_{\rm vir}$ defined by a value $\Delta_{\rm vir}$ from the spherical collapse model.

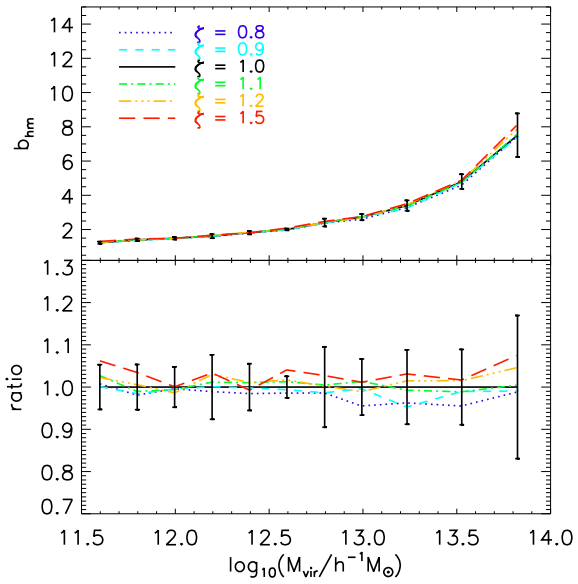

FIG. 7: Same as Fig. 4 but for the virial halo mass $M_{\rm vir}$ defined by a value $\Delta_{\rm vir}$ from the spherical collapse model.

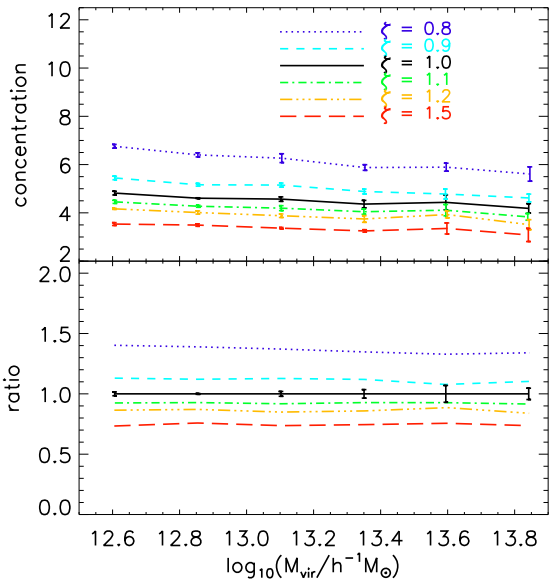

FIG. 6: Same as Fig. 3 but for the virial halo mass $M_{\rm vir}$ defined by a value $\Delta_{\rm vir}$ from the spherical collapse model.

started from the same initial condition. The redshifts for different ζ of the comparison of halo properties are selected when they have the same linear power spectrum as ΛCDM simulations at $z_S = 1.2$.

Based on our various comparisons, we summarize our findings as follows.

- The measured halo mass functions can differ from that in GR by about 5−10% for 10% deviation from GR ($|\zeta - 1| = 0.1$). Although the difference must be symmetric with respect to $\zeta = 1$ in the limit $\zeta \to 1$, it already shows significant asymmetry for $|\zeta - 1| \sim 10\%$. For example, the difference between the halo mass function of $\zeta = 0.9$ and that of GR is about twice of the corresponding case of $\zeta = 1.1$.

- For a 10% deviation from GR($|\zeta - 1| = 0.1$), the deviation of halo concentration can differ by 10−20%, which shows that modified gravity can significantly affect the structure formation on small scale and the internal properties of the dark matter halos.

- The halo bias is less sensitive to the nature of gravity. For all the $\zeta \neq 1$ values used in our simulation ($0.8 \leq \zeta \leq 1.5$), the halo bias differ from that of GR by less than 10%.

We note that all the above findings are obtained based on the halos that are defined to be the spherical over-density regions within which the average over-density are $\Delta_{200} = 200$ times the mean density $\rho_{\rm mean}$ of the universe. This definition is widely used in literature and is easy to be implemented both in simulations and in observations. The impact of using different Δ has been discussed using high resolution N-body simulations[37].

One might argue that the differences between MG models and the GR shown above are mainly due to the definition of the halos. To test to what extent halo definition impacts our results, we have also compared the halo mass function, concentration and bias using the virial halo mass $M_{\rm vir}$ (defined by a value $\Delta_{\rm vir}$ [31] from the spherical model) instead of M_{200}. According to the virial mass definition from GR, we do see in Fig. 5 that for a 20% deviation from ($|\zeta - 1| < 0.2$), the deviation of halo mass function differs by less than 10%, which is smaller

than that of the halo mass M_{200}. However, we can still detect the observed differences of the halo mass functions for different ζ values.

In Fig. 6, for $\zeta > 1.0$, the difference of $c_{\rm vir}(\zeta)$ with respect to that of GR is roughly the same as the case of $c_{200}(\zeta)$. Since at redshift $z_S = 1.2$, the universe is dominated by dark matter and R_{200} is approximately equal to $R_{\rm vir}$, which is 195.7 for our adopted parameters. In one word, by comparing the results shown in Fig. 3 and Fig. 6, we can see that there exists a significant difference of the halo concentration for different ζ values, which illustrates that deviations from general relativity can strongly affect the mass distribution in the nonlinear regime, although the large-scale structures are remarkably similar (see Fig. 1) [53].

Fig. 7 shows that the bias of halos defined with virial mass still shows weak dependence on gravity, for all the $\zeta \neq 1$ considered ($0.8 \leq \zeta \leq 1.5$). This confirmes previous finding that the halo bias may not be a sensitive probe of gravity. This conclusion would be robust for halos of mass less than $10^{13}\,h^{-1}{\rm M}_\odot$. Neverthless, our simulations do not have sufficiently large box size to robustly measure the bias of halos with mass larger than $10^{13}\,h^{-1}{\rm M}_\odot$ and evaluate its dependence on gravity.

In th above results $\Delta_{\rm vir}$ is evaluated assuming GR. It is known that $\Delta_{\rm vir}$ is changed in MG models [14, 40]. To what extent it can account for the found difference in the mass function [14, 40] is an issue for further investigation.

Our results have robustly demonstrated that the halo mass function is not completely determined by the shape and amplitude of the linear power spectrum. As a consequence, it shows significant dependence on the nature of gravity. We also show that the halo concentration is also affected by gravity. These results can be used to understand the impact of gravity on halo formation and distribution. They can also be used in halo model to understand the nonlinear matter clustering [20].

Acknowledgments

We would like to thank Volker Springel for the N-GenIC, Postprocessing code and detailed help. We are grateful to the anonymous referee for useful comments that helped to improve the presentation of this paper. Youcai thanks Donghai Zhao for helpful discussions. This work is supported by the national science foundation of China (grant Nos. 10973027, 11025316, 10973018, 10925314, 11233005, 11121062, 11203054), National Basic Research Program of China (973 Program) under grant No.2009CB24901, the CAS/SAFEA International Partnership Program for Creative Research Teams (KJCX2-YW-T23) and the Shanghai Committee of Science and Technology, China (grant No. 12ZR1452800).

[1] T. Narikawa and K. Yamamoto, 2012, JCAP, 5, 16
[2] D. B. Thomas and C. R. Contaldi, 2011, JCAP, 12, 13
[3] D. B. Thomas and C. R. Contaldi, 2011, arXiv:1112.6378
[4] B. Sartoris, S. Borgani, , P. Rosati, and J. Weller, 2011, arXiv:1112.0327
[5] B. Li, G.-B. Zhao, and K. Koyama, 2011, arXiv:1111.2602
[6] L. Lombriser, F. Schmidt, T. Baldauf, et al. 2011, arXiv:1111.2020
[7] D. S. Y. Mak, E. Pierpaoli, F. Schmidt, and N. Macellari, 2011, arXiv:1111.1004
[8] Y. Li and W. Hu, 2011, Phys. Rev. D , 84, 084033
[9] B. Jain and J. VanderPlas, 2011, JCAP, 10, 32
[10] M. Li, X-D. Li, S. Wang, and Y. Wang, 2011, Communications in Theoretical Physics, 56, 525
[11] S. W. Allen, A. E. Evrard, and A. B. Mantz, 2011, ARA&A, 49, 409
[12] T. Clifton, P. G. Ferreira, A. Padilla, and C. Skordis, 2011, arXiv:1106.2476
[13] S. Ferraro, F. Schmidt, and W. Hu, 2011, Phys. Rev. D , 83, 063503
[14] F. Schmidt, M. Lima, H. Oyaizu, and W. Hu, 2009, Phys. Rev. D , 79, 083518
[15] F. Schmidt, A. Vikhlinin, and W. Hu, 2009, Phys. Rev. D , 80, 083505
[16] G.-B. Zhao, B. Li, and K. Koyama, 2011, Physical Review Letters, 107, 071303
[17] B. Jain and J. Khoury, 2010, AnPhy, 325, 1479
[18] Y. P. Jing, H. J. Mo, and G. Boerner, 1998, Astrophys. J. , 494, 1
[19] A. Cooray and R. Sheth, 2002, Physics Report, 372, 1
[20] W. Cui, P. Zhang, and X. Yang, 2010, Phys. Rev. D , 81, 103528
[21] H. Oyaizu, 2008, Phys. Rev. D , 78, 123523
[22] H. Oyaizu, M. Lima, and W. Hu, 2008, Phys. Rev. D , 78, 123524
[23] G.-B. Zhao, B. Li, and K. Koyama, 2011, Phys. Rev. D , 83, 044007
[24] F. Schmidt, 2009, Phys. Rev. D , 80, 043001
[25] K. C. Chan and R. Scoccimarro, 2009, Phys. Rev. D , 80, 104005
[26] B. Li, G.-B. Zhao, R. Teyssier, and K. Koyama, 2012, JCAP, 1, 51
[27] V. Springel, 2005, MNRAS, 364, 1105
[28] M. Davis, G. Efstathiou, C. S. Frenk, and S. D. M. White, 1985, Astrophys. J. , 292, 371
[29] Z. Lukić, D. Reed, S. Habib, and K. Heitmann, 2009, Astrophys. J. , 692, 217
[30] J. F. Navarro, C. S. Frenk, and S. D. M. White, 1997, Astrophys. J. , 490, 493
[31] V. R. Eke, S. Cole, and C. S. Frenk, 1996, MNRAS, 282, 263
[32] W. H. Press and P. Schechter, 1974, Astrophys. J. , 187, 425
[33] J. R. Bond, S. Cole, G. Efstathiou, and N. Kaiser, 1991, Astrophys. J. , 379, 440
[34] R. K. Sheth and G. Tormen, 1999, MNRAS, 308, 119
[35] A. Jenkins, C. S. Frenk, , S. D. M. White, J. M. Col-

berg, S. Cole, A. E. Evrard, H. M. P. Couchman, and N. Yoshida, 2001, MNRAS, 321, 372
[36] M. S. Warren, K. Abazajian, D. E. Holz, and L. Teodoro, 2006, Astrophys. J. , 646, 881
[37] J. Tinker, A. V. Kravtsov, A. Klypin, K. Abazajian, M. Warren, G. Yepes, S. Gottlöber, and D. E. Holz, 2008, Astrophys. J. , 688, 709
[38] S. Bhattacharya, K. Heitmann, M. White, et al. 2011, Astrophys. J. , 732, 122
[39] W. Cui, M. Baldi, and S. Borgani, 2012, arXiv:1201.3568
[40] F. Schmidt, W. Hu, and M. Lima, 2010, Phys. Rev. D , 81, 063005
[41] R. K. Sheth, H. J. Mo, and G. Tormen, 2001, MNRAS, 323, 1
[42] Y. P. Jing and Y. Suto, 2000, ApJ, 529, L69
[43] J. S. Bullock, T. S. Kolatt, Y. Sigad, R. S. Somerville, A. V. Kravtsov, A. A. Klypin, J. R. Primack, and A. Dekel, 2001, MNRAS, 321, 559
[44] D. H. Zhao, H. J. Mo, Y. P. Jing, Y. P., G. Börner, 2003, MNRAS, 339, 12
[45] A. F. Neto, et al. 2007, MNRAS, 381, 1450
[46] D. H. Zhao, Y. P Jing, H. J. Mo, G. Börner, 2009, Astrophys. J. , 707, 354
[47] A. Jeeson-Daniel, C. Dalla Vecchia, M. R. Haas, and J. Schaye, 2011, arXiv:1103.5467
[48] H. J. Mo, and S. D. M. White, 1996, MNRAS, 282, 347
[49] U. Seljak and M. S. Warren, 2004,MNRAS, 355, 129
[50] J. L. Tinker, B. E. Robertson, A. V. Kravtsov, et al. 2010, Astrophys. J. , 724, 878
[51] Strictly speaking, MG described by a spatial and time dependent ζ is still environmental independent. Nevertheless, ζ with spatial and time dependence is promising to mimic the statistically averaged properties of a environmental dependent MG model. In such case, the interpretation of ζ may not be straightforward.
[52] A calculator which allows one to interactively generate data for any given cosmological model is provided at http://www.shao.ac.cn/dhzhao/mandc.html.
[53] This behavior should also hold for more realistic modified gravity models with screening mechanisms required to pass the solar system tests. In this case, the halo center may be well shielded. Nevertheless, the accretion history and the halo outskirts are impacted by modifications to GR.